

Original Research

# Infection of Human Macrophage-Like Cells by African Swine Fever Virus

Zaven A. Karalyan<sup>1,\*</sup>, Susanna A. Ghonyan<sup>2</sup>, Davit A. Poghosyan<sup>2</sup>, Lina H. Hakobyan<sup>1</sup>, Hranush R. Avagyan<sup>1,3</sup>, Aida S. Avetisyan<sup>1,3</sup>, Liana O. Abroyan<sup>1</sup>, Arpine A. Poghosyan<sup>1</sup>, Sona A. Hakobyan<sup>1</sup>, Gayane P. Manukyan<sup>2</sup>

<sup>1</sup>Laboratory of Cell Biology and Virology, Institute of Molecular Biology of NAS RA, 0014 Yerevan, Armenia

<sup>2</sup>Laboratory of Molecular and Cellular Immunology, Institute of Molecular Biology NAS RA, 0014 Yerevan, Armenia

<sup>3</sup>Experimental Laboratory, Yerevan State Medical University after M. Heratsi, 0025 Yerevan, Armenia

\*Correspondence: [zkaralyan@yahoo.com](mailto:zkaralyan@yahoo.com) (Zaven A. Karalyan)

Academic Editor: Ananda Ayyappan Jaguva Vasudevan

Submitted: 21 September 2023 Revised: 15 January 2024 Accepted: 18 February 2024 Published: 23 April 2024

## Abstract

**Background:** The African swine fever (ASF) virus (ASFV) and ASF-like viral sequences were identified in human samples and sewage as well as in different water environments. Pigs regularly experience infections by the ASFV. The considerable stability of the virus in the environment suggests that there is ongoing and long-term contact between humans and the ASFV. However, humans exhibit resistance to the ASFV, and the decisive factor in developing infection in the body is most likely the reaction of target macrophages to the virus. Therefore, this study aimed to characterize the responses of human macrophages to the virus and explore the distinct features of the viral replication cycle within human macrophages. **Methods:** The ASFV Armenia/07 strain was used in all experiments. In this study, quantitative real-time polymerase chain reaction (qRT-PCR) was used to determine the ASFV gene expression; flow cytometry analysis was performed to evaluate the effects of the inactive and active ASFV (inASFV and aASFV) treatments on the phenotype of THP-1-derived macrophages (M $\phi$ 0) and inflammatory markers. Moreover, other methods such as cell viability and apoptosis assays, staining techniques, phagocytosis assay, lysosome-associated membrane protein (LAMP-1) cytometry, and cytokine detection were used during experiments. **Results:** Our findings showed that the virus initiated replication by entering human macrophages. Subsequently, the virus shed its capsid and initiated the transcription of numerous viral genes, and at least some of these genes executed their functions. In THP-1-derived macrophages (M $\phi$ 0), the ASFV implemented several functions to suppress cell activity, although the timing of their implementation was slower compared with virus-sensitive porcine alveolar macrophages (PAMs). Additionally, the virus could not complete the entire replication cycle in human M $\phi$ 0, as indicated by the absence of viral factories and a decrease in infectious titers of the virus with each subsequent passage. Overall, the infection of M $\phi$ 0 with the ASFV caused significant alterations in their phenotype and functions, such as increased TLR2, TLR3, CD80, CD36, CD163, CXCR2, and surface LAMP-1 expression. Increased production of the tumor necrosis factor (TNF) and interleukin (IL)-10 and decreased production of interferon (IFN)- $\alpha$  were also observed. Taken together, the virus enters human THP-1-derived macrophages, starts transcription, and causes immunological responses by target cells but cannot complete the replicative cycle. **Conclusion:** These findings suggest that there may be molecular limitations within human macrophages that at least partially restrict the complete replication of the ASFV. Understanding the factors that hinder viral replication in M $\phi$ 0 can provide valuable insights into the host–virus interactions and the mechanisms underlying the resistance of human macrophages to the ASFV.

**Keywords:** African swine fever virus; THP-1-derived human macrophages; gene transcription; cytometry; TLRs; LAMP-1

## 1. Introduction

The high frequency of human contact with domestic pigs poses a significant risk for transmitting the African swine fever virus (ASFV) to humans. Although the ASFV primarily affects members of the Suidae family, similar genomes or ASFV-like sequences have been isolated from various samples of human biological materials, including serum and water environments [1,2]. The entry of such viruses into the human body most likely occurs through the alimentary route and does not cause infection. It is known that the ASFV cannot infect or cause disease in humans, even in regions where the virus is endemic. However, the

identification of ASFV-like sequences in the serum of several human patients suggests that human infection may be possible [1].

Porcine (primary) macrophages, including porcine alveolar macrophages (PAMs), are the main target of the ASFV. The virus developed several strategies to replicate efficiently, avoiding recognition by the host immune system [3]. For the first time, the ability of the ASFV to affect non-porcine macrophages (M $\phi$ 0) was initially investigated in 1977 [4]. The study revealed that M $\phi$ 0 macrophages, infected with the VERO cell-adapted ASFV, demonstrated an intense ability to destroy the cells. The lat-



ter was not associated with either virus propagation or induction of DNA synthesis [4]. At the same time, the authors pointed to an abortive replication of the ASFV in chicken macrophages. The authors speculated that one possible explanation for this phenomenon could be the possibility of division (progress to the cell cycle) in chicken macrophages. Few studies also report successful adaptation of the wild-type ASFV strains to continuous cell lines of human origin [5,6]. However, there are significant differences between replication in actively dividing cell lines and macrophages, usually in the G0 phase of the cell cycle. Macrophages typically exist in two states, G0 and G1-like states, rather than in the S and/or G2 phases of the cell cycle [7]. The significance of cell cycle progress for ASFV replication was also shown on virus-sensitive (PAMs). Based on the findings of Avagyan *et al.* [8] 2022, it is highly probable that the stimulation of the cell cycle in infected PAMs is necessary for ASFV replication to acquire the necessary nucleotides.

Given the central importance of macrophages in controlling the pathogenesis of viral infections, including the ASFV, we aimed to investigate the ability of the ASFV to adapt and replicate in human macrophages. Specifically, we sought to understand the mechanisms that limit the susceptibility of M $\phi$ 0 (M0 macrophages) to the ASFV. To address these questions, we conducted *in vitro* infections of THP-1-derived M0 macrophages with the ASFV. This model allowed us to assess the phenotypic and functional changes in M0 macrophages induced by the viral load and examine the replication of the virus within the cells.

## 2. Materials and Methods

### 2.1 The Virus

The ASFV Armenia/07 strain was used in all experiments. The ASFV was obtained from the spleen of infected pigs. The virus (Armenia/07) was first isolated in 2007 from the spleen of an ASFV-infected swine. Virus titration was performed as described previously and expressed by hemadsorption unit (HADU) as lg10 HADU50/mL for non-adapted cells [9]. Measurements in HADU make it possible to estimate the number of infectious units of the virus when studying hemadsorbing strains of the ASF virus. Therefore, this technique complements quantitative measurements of viral genome copies well. The titer was expressed as hemadsorption units—an HADU50/mL.

The virus for experiments was received after 48 h infections of PAMs. The HADU technique was carried out on the primary culture of porcine alveolar macrophages [10]. The ASFV was inactivated by incubating in a water bath (65 °C at 10 min). After heat inactivation, the virus was tested for infectivity using *in vitro* cell culture.

### 2.2 Cell Culture

All the information about software/equipment/drugs/reagents are included in **Supplementary Material 1**. Human acute myeloid leukemia

cell line THP-1 obtained from ATCC (Manassas, VA, USA), validated by STR profiling and tested negative for mycoplasma, was maintained in RPMI 1640 (Life Technologies) medium and supplemented with 10% heat-inactivated fetal bovine serum, 2 mM L-glutamine, 10 mM Hepes, and 100 U/mL penicillin, 100  $\mu$ g/mL streptomycin (Sigma) in a humidified incubator at 37 °C with 5% CO<sub>2</sub>. M0 macrophage-like THP-1 cells (M $\phi$ 0) were generated in a 24-well plate at a density of  $2 \times 10^5$  cells per milliliter by the treatment of THP-1 cells with phorbol 12-myristate 13-acetate (PMA) for 72 h, followed by a resting period in fresh RPMI medium for 24 h. The plates were washed with RPMI to remove non-adherent cells before other experimental viral treatments. Polarized M0 status was confirmed by flow cytometry and microscopy.

### 2.3 Human Macrophage Infection

For *in vitro* experiments, ASFV was grown in a culture of THP-1-derived M0 macrophages (M $\phi$ 0) for 24 h and 48 h. M $\phi$ 0, seeded as described above, were inoculated with ASFV Arm07 at  $10^4$  HADU50/mL from the 1st passage; the dose was chosen to prevent spontaneous apoptosis caused by viral particles (0,1 MOI). Following adsorption at 37 °C for 1 h, the infected cell monolayer was washed twice to remove any unbound viruses. A complete medium was then added and analyzed at the indicated time points. The ASFV infection was performed on M $\phi$ 0 in two stages—24 hours post-infection (hpi) and 48 hpi. After 1 hpi, cells were washed twice with medium and cultivated at 37 °C with 5% CO<sub>2</sub> [9].

### 2.4 Porcine Alveolar Macrophages Infection

For comparison with human macrophages, we used a primary culture of PAMs, which were seeded according to the generally accepted standard method and inoculated with ASFV Arm07 at  $10^4$  HADU50/mL. After adsorption at 37 °C for 1 h, the infected cell monolayers were washed twice to remove unbound viruses. Afterward, a complete medium was added and analyzed at the indicated time. All data were obtained at 24 and 48 hpi [9].

### 2.5 Cell Viability and Apoptosis Assays

Macrophage apoptosis and viability during infection were assessed using Annexin V and propidium iodide (PI). The cells were harvested, trypsinized, and resuspended in Annexin binding buffer before adding 5  $\mu$ L Annexin V-FITC (Biolegend) and incubated in the dark at 4 °C for 30 min. Immediately before cytometric analysis, the cells were labeled with PI. Data were acquired on a FACS Calibur (BD Biosciences) and analyzed using the FlowJo vX0.7 software (Tree Star, Inc., San Carlos, CA, USA).

### 2.6 Staining Techniques

To better characterize cellular morphology, investigated cells were cultured in 6-well chamber slides. For

**Table 1. Details of oligonucleotide primers employed in the quantitative real-time polymerase chain reaction (qRT-PCR) assay.**

Gene	Product	Sequence (5'-3')
<i>F778R</i>	Ribonucleotide reductase	F: TATGAACCTGAACTAAGC R: AATGACAGTAATAGGAACC
<i>F334L</i>	Ribonucleotide reductase	F: CAATCATCAATGTCCTTAC, R: GAATGTTGGAACCTGGTAT
<i>E165R</i>	dUTPase	F: CCTGACCATATCAACATCCTAA R: AATCTACCCTCGCCTCTT
<i>G1112R</i>	DNA polymerase	F: CCGACTCATTATACATTACAT R: TCATAGACAGAAGCACTT
<i>P1192R</i>	II DNA topoisomerase	F: TGAAGAGCAAGATTCCATAGA R: <i>GTAAGGTAGCCACGCATA</i>
<i>A240L</i>	Thymidylate kinase	F: TCGTGTGGAATACTCATTG R: TCGTGTCTGGATTAGGAA
<i>K196R</i>	Thymidine kinase	F: GCAGTTGTCGTAGATGAAG R: CGAAGGAAGCATTGAGTC
<i>F1055L</i>	Helicase Superfamily II	F: TTGAAGAAGTGCCTGATA R: ATAGAATTATTGCCGTAGTATT
<i>B246L</i>	<i>P72</i>	F: CCGATCACATTACCTCTTATTAACAAACATTTC R: GTGTCCCAACTAATAAAAATCTCTTGCTCT
<i>R298L</i>	Serine/threonine-protein kinase	F: GTGTGGACGATAGGTATGG R: TCTGAAATGTTCTCGGGAAT
<i>EP1142L</i>	DNA-directed RNA polymerase subunit beta	F: ATCAATAGCACCAAGTTCTCA R: TGTCATCGCCTGTCATTC
<i>0174L</i>	DNA polymerase X-like	F: CATCGTTGCTGTTGGTAG R: TCCTTTATGCGAATGTTGG
<i>A859L</i>	Helicase	F: CCTTCTCTTCTGTGATTG R: GACATTCATCGCTAATAATAAG

morphological analysis, cells were fixed in pure methanol and stained with Pappenheim (Cypress Diagnostics, Belgium), according to the manufacturer's protocol. Additionally, Hematoxylin–Eosin staining was used (Sigma-Aldrich, Germany), according to the manufacturer's protocols.

To detect viral factories, cytospectrophotometry and Feulgen–Naphthol Yellow S staining procedures were used as described previously [11].

### 2.7 Flow Cytometry

Flow cytometry analysis was used to evaluate the effect of inactive and active ASFV (inASFV and aASFV) treatments on Mφ0 phenotype and inflammatory markers. At the end of each experiment, the cells were washed twice and incubated for 15 min with PBS supplemented with 1% bovine serum albumin (BSA) to prevent non-specific binding of antibodies and conjugated with the following antibodies: CD36-FITC, CD80-FITC, CD163-PE, CD11b-PerCP, HLA-DR-PerCP, CD11b-PerCP, CD282 (TLR2)-Pe-Cy7, CD182 (CXCR2)-PeCy7, CDD197 (CCR7)-APC, CD11c-APC-Cy7, and CD14-APC-Cy7. To analyze the intracellular expression of the TLRs, the cells were fixed and permeabilized after surface-staining and labeled with

CD283 (TLR3)-PE and CD289 (TLR9)-APC (all Biolegend). Positive and negative thresholds for fluorescence signals were defined using isotype-specific negative controls. Data were acquired on a Becton Dickinson LSRII flow cytometer and analyzed using the FlowJo vX0.7 software. In all experiments, a minimum of 10,000 events were counted. Results are expressed as the percentage and mean fluorescence intensity (MFI).

### 2.8 Phagocytosis Assay

For determining the phagocytic capacity of macrophages, pH-sensitive fluorochrome pHrodo-green-labeled Zymosan BioParticles (ThermoFisher) were used at a concentration of 50 µg/mL, according to the manufacturer's recommendation. Briefly, particles were added to the attached cells and incubated at 37 °C and 5% CO<sub>2</sub> for 2 h. All cell lines were validated by STR profiling and tested negative for mycoplasma. Cells were all cultured in a humidified incubator at 37 °C and 5% CO<sub>2</sub>. Cells were placed on ice to stop further phagocytosis and analyzed using a FACS Calibur (BD Biosciences). The frequency of pHrodo+ cells and/or the mean fluorescence intensity (MFI) was determined.

## 2.9 LAMP-1 Cytometry

After the indicated stimulations, the cells were removed from the plate by trypsinization, washed, and stained with surface lysosome-associated membrane protein (LAMP-1-PE, CD107a). Then, the cells were fixed, permeabilized, and stained with LAMP-1-APC (Biolegend) for intracellular staining. Afterward, the cells were washed and analyzed by flow cytometry.

## 2.10 Cytokine Detection

After the treatments described above, cell-free supernatants were quantified for the presence of interleukin (IL)-10, tumor necrosis factor (TNF), and interferon (IFN)- $\alpha$  using an enzyme-linked immunosorbent assay (Biolegend), according to the manufacturer's protocols. Absorbance was read at 450 nm using a HiPo MPP-96 Plate Reader.

## 2.11 Gene Expression Analysis by Quantitative Real-Time PCR

To determine ASFV expression in PAM cell lines, total viral RNA/DNA was isolated using the HiGene™ Viral RNA/DNA Prep kit (BIOFACT). RNA/DNA samples were then reverse transcribed using the FIREScript® RT cDNA synthesis kit (Solis Biodyne). Both methods were conducted following the manufacturer's instructions. When measuring DNA/RNA concentrations with a NanoDrop® ND-1000, UV-Vis Spectrophotometer A260/280 values were acceptable. A ratio of ~1.8 is considered "pure" for DNA; a ratio of ~2.0 is considered "pure" for RNA. Quantitative real-time PCR was performed using the SYBR green methods previously described [12,13] on an Eco Illumina Real-Time PCR system device (Illumina Inc). Each reaction mixture (20  $\mu$ L) was composed of 4  $\mu$ L of 5 $\times$  HOT FIREPol® EvaGreen® qPCR Mix Plus (ROX) (Solis Biodyne), 0.2  $\mu$ L of each specific primer, 4  $\mu$ L of template DNA/cDNA, and 11.6  $\mu$ L of ddH<sub>2</sub>O. Positive and negative controls were used. DNA isolated from an ASFV-infected pig's spleen was used as a positive control. For the negative control, ddH<sub>2</sub>O was added to the reaction mix instead of a sample. Reactions were carried out in the following conditions: polymerase activation: 95 °C for 12 min, 40 cycles: 95 °C for 15 s, 52 °C for 30 s, and 72 °C for 30 s. Standard curves were created using serial 10-fold dilutions of viral DNA. The fluorescence threshold value (Ct) was calculated using the ECO-Illumina system software. Primers used for amplification were designed and ordered from Integrated DNA Technology-IDT (<https://www.idtdna.com/pagesasfollows>).

Viral genes were measured at 48 hpi to determine the viral amount and after 24 hpi to analyze the transcriptional activity of separate genes. For alignment of the cDNA plots and infection titers of ASFV, Cq values were rescaled after comparing with viral genome copies and modified in absolute amounts along the y-axis for better visualization. To evaluate the ASFV replication effectivity profile, the genes

with different temporal expression patterns were identified [8,14]. All primers are listed in Table 1.

## 2.12 Enzyme-Linked Immunosorbent Assay

Porcine IFN- $\alpha$  (MBS162596), IL-10 (MBS2019681), and TNF- $\alpha$  (MBS2019932) were purchased from MyBioSource. ELISA was performed using the manufacturer's description. The IFN levels and/or receptors were measured in duplicate using a colorimetric reader (Stat Fax 303 Plus) and calculated according to the standard curve supplied by the kit.

## 2.13 Statistical Analysis

Statistical analyses were performed using GraphPad Prism software (version 6.01, <https://www.graphpad.com/scientific-software/prism/www.graphpad.com/scientific-software/prism/>). The results are expressed as the mean  $\pm$  standard error (SEM). Statistical significance for the differences between groups measured in M $\phi$ 0 cells was calculated using one-way ANOVA with Tukey's multiple comparisons test. \* $p < 0.05$ , \*\* $p < 0.01$ .

All *in vitro* experiments with virus analysis were conducted in triplicate. The significance has been evaluated using a two-tailed Student's *t*-test. SPSS version 17.0 (SPSS Inc., Chicago, IL, USA) has been applied for statistical analyses.

# 3. Results

## 3.1 Passaging of ASFV on Human Macrophage-Like Cells

The virus was blindly passaged to determine the possible susceptibility of M $\phi$ 0 to ASFV infection. We found that the genome copies of ASFV decreased in M $\phi$ 0 starting from the first passage to the fourth (Fig. 1A). The *K196R* gene belongs to the group of late genes. Since the late genes in the ASF virus in an unusual target cell are not always transcribed or transcribed very late, we chose one of the late genes to better assess the virus's ability to replicate fully. However, simultaneously with the *K196R* gene, we also studied other genes that showed similar results (data not shown). Similar data were obtained when the virus was titrated by HADU (Fig. 1B). The number of infectious virus particles at the third passage was 2.5–3 lg lower than the initial one and stock virus. However, the ASFV was detected in all examined samples in the third passage. In the fourth passage, only one of the six samples contained an infectious virus (Fig. 1B). Despite this, transcription of some viral genes continued (or persisted) in the third passage, although it had almost disappeared in the fourth passage (Fig. 1A).

## 3.2 Comparison of Transcriptional Activity of ASFV Early and Late Genes in Infected Human Macrophage-Like Cells

We studied thirteen genes involved in viral replication to identify and analyze the transcriptional activity of the ASFV genes in human M $\phi$ 0 cells. The level of the virus genes was compared with the viral transcript levels. All

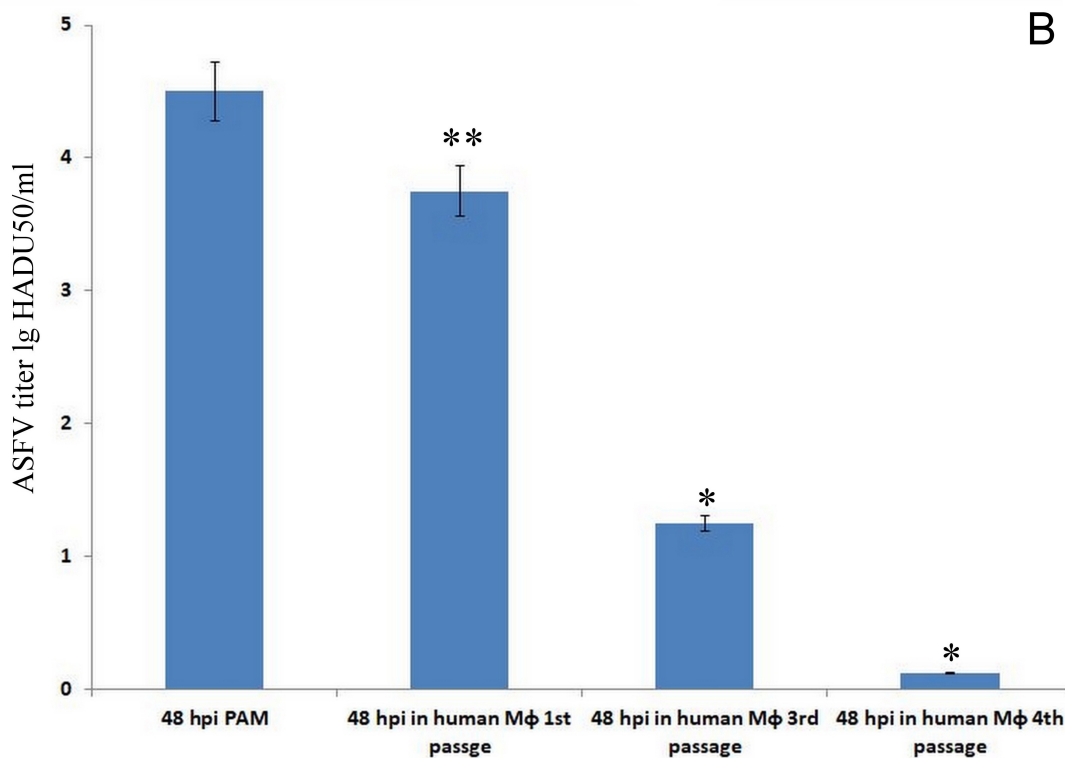
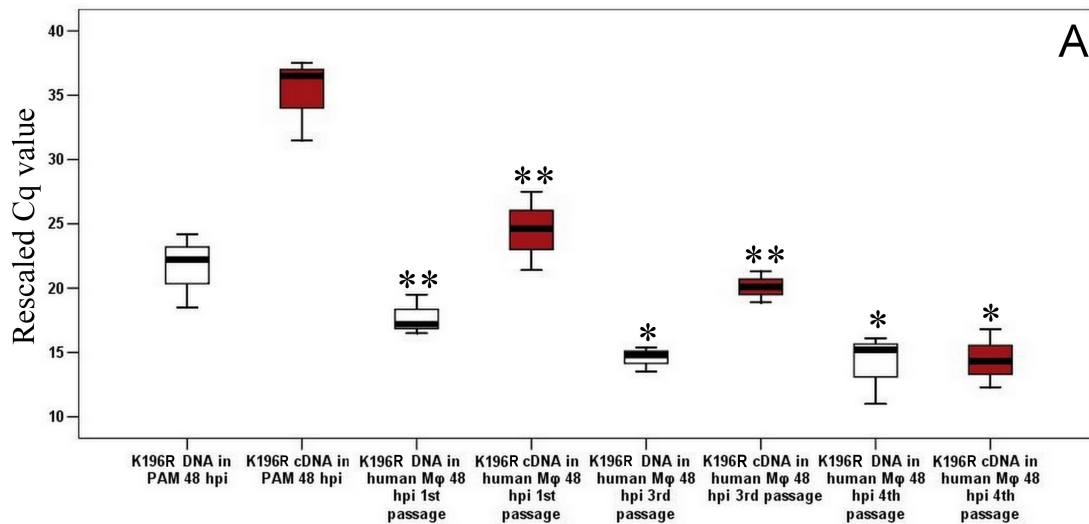


**Fig. 1. African swine fever virus (ASFV) amounts in porcine alveolar and human macrophages.** (A) Quantitative real-time polymerase chain reaction (PCR) results of genome amount ASFV K196R and complementary DNA (cDNA) in 1st, 3rd, and 4th passages. \*significant compared with 1st passage ( $p < 0.05$ ); \*\* tendency ( $p < 0.1$ ) compared with 1st passage. (B) ASFV hemadsorption unit (HADU) titers in  $M\phi$  in 1st, 3rd, and 4th passages. \*significant compared with porcine alveolar macrophage (PAM) ( $p < 0.05$ ); \*\* tendency ( $p < 0.1$ ) compared to PAM.

studied genes were divided into two groups: early genes (Fig. 2A) and ambivalent to replication time genes—late genes (Fig. 2B).

The following ASFV early genes can be transcribed in  $M\phi$  cells: *F778R* ribonucleotide reductase (large subunit), *F334L* ribonucleotide reductase (small subunit), *E165R* deoxyuridine triphosphatase, *G1211R* DNA polymerase  $\alpha$ -like, *P1192R* DNA topoisomerase type II. At the same time,

our data did not reveal the transcriptional activity of early genes, such as the *F1055L* helicase superfamily and *A240L* thymidylate kinase (Fig. 2A).

Ambivalent genes *O174L* DNA polymerase X-like and *K196R* thymidine kinase exhibited transcriptional activity, whereas *EPI242L* RNA polymerase subunit 2 and *A859L* helicase superfamily II did not display any detectable transcriptional activity. Both late genes *R298L* ser-

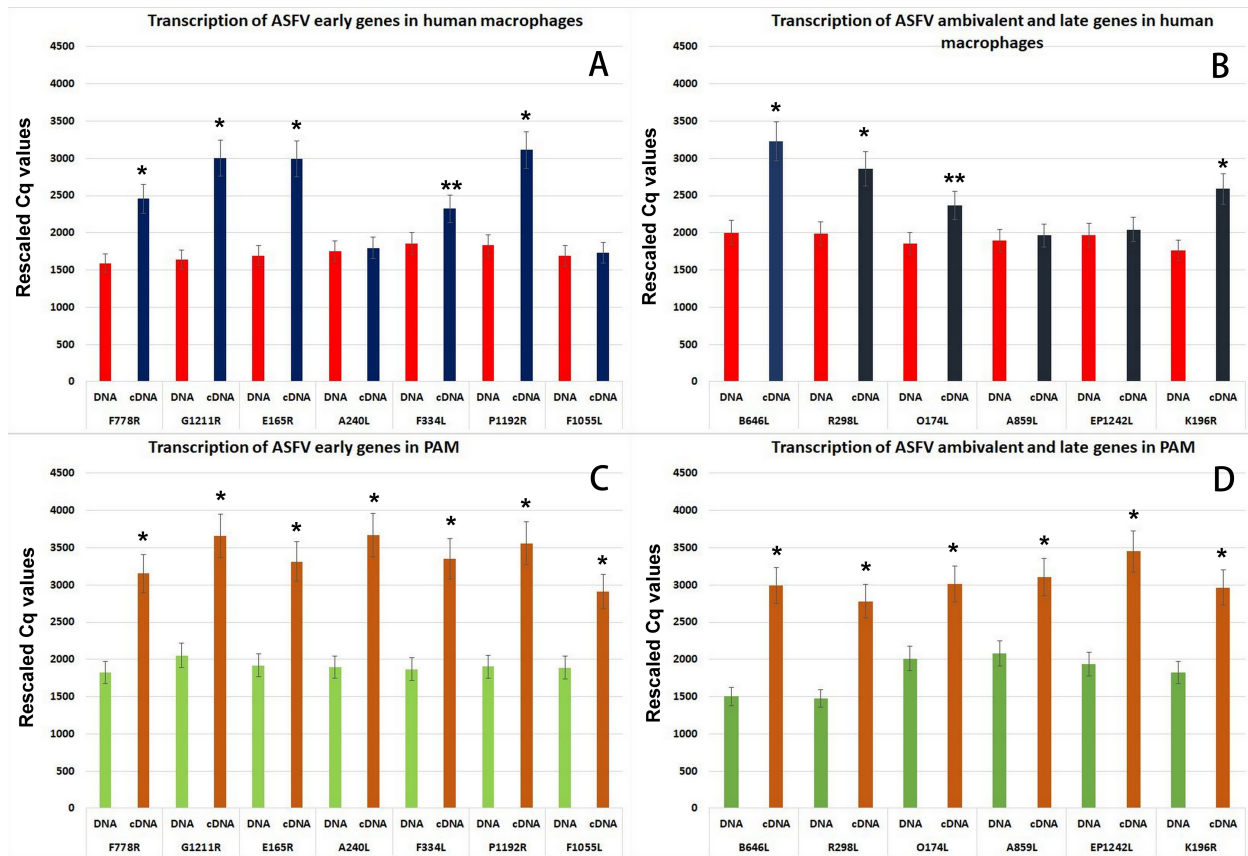


**Fig. 2. Quantitative real-time PCR results of ASFV *K196R*, *R298L*, *A2410L*, *F778R*, *F334L*, and *E165R* mRNA (cDNA) in ASFV-infected human  $M\phi 0$  and PAM lysates at 24 hpi.** (A) Early genes and their transcriptional activity (cDNA) in ASFV-infected  $M\phi 0$ . (B) Ambivalent and late genes and their transcriptional activity (cDNA) in ASFV-infected  $M\phi 0$ . (C) Early genes and their transcriptional activity (cDNA) in ASFV-infected PAMs. (D) Early genes and their transcriptional activity (cDNA) in ASFV-infected PAMs. \*significant compared to PAMs ( $p < 0.05$ ); \*\* tendency ( $p < 0.1$ ) compared to DNA levels. mRNA, messenger RNA;  $M\phi 0$ , M0 macrophages; hpi, hours post infection.

ine protein kinase and *B646L* major capsid protein demonstrate transcriptional activity (Fig. 2B). In conclusion, regardless of the timing of transcription in susceptible cells, certain ASFV genes show transcriptional activity, and others do not.

The same genes were examined for transcriptional activity in PAMs infected with a similar dose of ASF virus. As follows from Fig. 2, all genes, both early (Fig. 2C) and late (Fig. 2D), demonstrate high transcriptional activity.

### 3.3 Morphological Examination

A morphological examination revealed that intact macrophages generally have a small and round shape, with few vacuoles and small pseudopodia. Nonetheless, signs of macrophage activation can occasionally be detected within the intact population. Additionally, intact macrophages were also characterized by cytoplasmic vacuolization, which was observed only in a minority of cells (Fig. 3A).

Analysis of the morphology of  $M\phi 0$  cells infected with the virus showed noteworthy variations at 24 and 48

hpi. At 24 hpi, the morphology of macrophages infected with the inactivated virus resembled that of macrophages infected with the active virus, possibly due to viral envelope components. Both groups of infected  $M\phi 0$  cells exhibited prominent cytoplasmic vacuolization, which occupied most of the volume of the cytoplasm and sometimes the nucleus (Fig. 3B). Cytoplasmic vacuolization and basophilia were typically absent in intact macrophages (Fig. 3A), they were observed in  $M\phi 0$  cells infected by both inactivated and active virus (Fig. 3C,D). By 48 hpi, significant differences were observed between the two groups with the inactivated virus, where macrophage activation continues in groups with the infectious virus (Fig. 3E,F), where many signs of inhibition of cell activity were observed. Pronounced pseudopodia were visible in some ASFV-infected  $M\phi 0$  cells (Fig. 3E).

Furthermore, it is worth mentioning that none of the samples analyzed for the presence of viral factories on Feulgen-stained preparations revealed DNA-positive structures in the cytoplasm of infected cells (Fig. 3G). In contrast, when ASFV infects susceptible cells, such as primary

cultures of PAMs, factories are typically detected in significant numbers and are clearly visible (Fig. 3H). Hence, M $\phi$ 0 infected with ASFV (Arm07) do not exhibit the typical factories observed in infected susceptible cells, such as PAMs.

### 3.4 Apoptotic Rate and Death of M $\phi$ 0 Transfected with ASFV

To investigate the viability of M $\phi$ 0 cells upon infection with ASFV, we analyzed the rates of dead cells and apoptosis. Flow cytometry analysis has shown that active and inactive viruses do not alter the viability of M $\phi$ 0 cells after infection for 48 hours. Despite the apoptotic rate being increased in both suited groups (aASFV and inASFV), their differences from the control group were not significant (Fig. 4A).

### 3.5 Phagocytic Activity of M $\phi$ 0 Cells and their Lysosomal Content

Next, we studied the phagocytic activity of ASFV-infected M $\phi$  with pH-sensitive fluorescent pHrodo dye. After engulfment, the intensity of pHrodo light emission was slightly elevated in M $\phi$ 0 infected with inASFV ( $p = 0.05$ ) compared to non-infected M $\phi$ 0 (Fig. 4B).

The analysis revealed low lysosomal membrane glycoprotein LAMP-1 expression at the M $\phi$ 0 surface. Both M $\phi$ 0+aASFV and M $\phi$ 0+inASFV exhibited increased surface LAMP-1, indicative of lysosome exocytosis of the marker on the cell surface. In opposition to the surface marker expression, intracellular expression of LAMP-1 showed decreased expression in both studied groups (not significant) (Fig. 4C).

### 3.6 Immunophenotype and TLR expression on M $\phi$ 0 cells

To elucidate the response of M $\phi$ 0 cells toward the presence of the ASFV, we characterized the phenotype of the cells. Histograms of a representative experiment and a summary of the surface marker expression profile for each studied group are shown in Fig. 5. Overall, flow cytometry analysis revealed that both aASFV and inASFV caused detectable changes in marker expression in M $\phi$ 0 cells. As shown in Fig. 5, the expression of several CD markers was upregulated by the cells infected with active virus (aASFV), namely CD36, CD163, CXCR2, and CD80. Interestingly, the expression of CD11c was downregulated in infected cells, which is indicative of cell activation, albeit not significantly. The process of downregulating the expression of CD11c is triggered by TLR4, TLR3, and TLR9 signaling [15].

Intending to identify cellular pattern recognition receptors (PRRs) responsible for the viral activation in macrophages, we examined the expression levels of TLR3 and TLR9, which have been described as receptors that mediate the sensing of the ASFV (Ayanwale *et al.* [16] 2022). TLR2 was analyzed as a receptor able to recognize viral antigens and sense endogenous danger-associated molecu-

lar patterns (DAMPs) to trigger the process of self-healing and tissue repair [17]. We found that TLR2 expression was slightly upregulated in both the inASFV and aASFV. Interestingly, the percentage of M $\phi$ 0 cells positive for TLR3 (receptor mediating sensing of ASFV) was significantly increased only in a group of the cells treated with the aASFV (Fig. 5).

### 3.7 Cytokine Production

Next, we measured the accumulation of TNF- $\alpha$ , IL-10, and IFN- $\alpha$  in culture supernatants of ASFV-infected M $\phi$ 0 cells (Fig. 6A). The induction of TNF- $\alpha$  resembled mainly immunophenotyping results. Production of IL-10 was significantly increased in the aASFV group compared with the inASFV group. Notably, the production of IFN- $\alpha$  was reduced by the active virus.

Similar to THP-1-derived M $\phi$ 0 cells, the levels of measured TNF- $\alpha$  were increased in the PAMs infected with ASFV, while the supernatant levels of IL-10 remained unchanged (Fig. 6B). However, the production of IFN- $\alpha$  differed between the THP-1-derived M $\phi$ 0 and PAMs. Particularly, PAMs infected with ASFV secreted higher amounts of IFN- $\alpha$  than the control group.

## 4. Discussion

Given the relative persistence of ASFV in the environment, humans have been in close contact with the virus for a long time; therefore, it is reasonable to assume that there have been numerous cases of human infection with the virus. Isolation of the ASFV-like virus genomes from various samples of human biological materials, including serum, confirms this fact [1]. There is also a study of the interaction of ASFV particles with rabbit macrophages, which linked the absence of specific receptors in these cells with the absence of a productive infection. Despite the aforementioned, no pathological changes have been identified in humans during an extensive virus screening. Only one known study describes an association between ASF infection and human-acquired immunodeficiency syndrome [18]. However, those studies did not have a strong evidence base and are disputed today. Given the previous, the human body has a high resistance to the ASFV.

It is important to note that the inhibition of transcriptional activity in M $\phi$ 0 infected with ASFV is not selective to only early or late genes but rather a non-selective inhibition of a number of genes from both categories [19,20]. This suggests that the virus is selectively inhibiting the transcriptional activity of certain genes, regardless of whether these are early or late genes. Further studies are required to elucidate the mechanisms of such selective inhibition of viral gene transcription.

The limited cell tropism of ASFV suggests that a macrophage-specific receptor is required for infection. Recent studies have suggested that CD163 may be necessary for infection but insufficient, suggesting other surface pro-

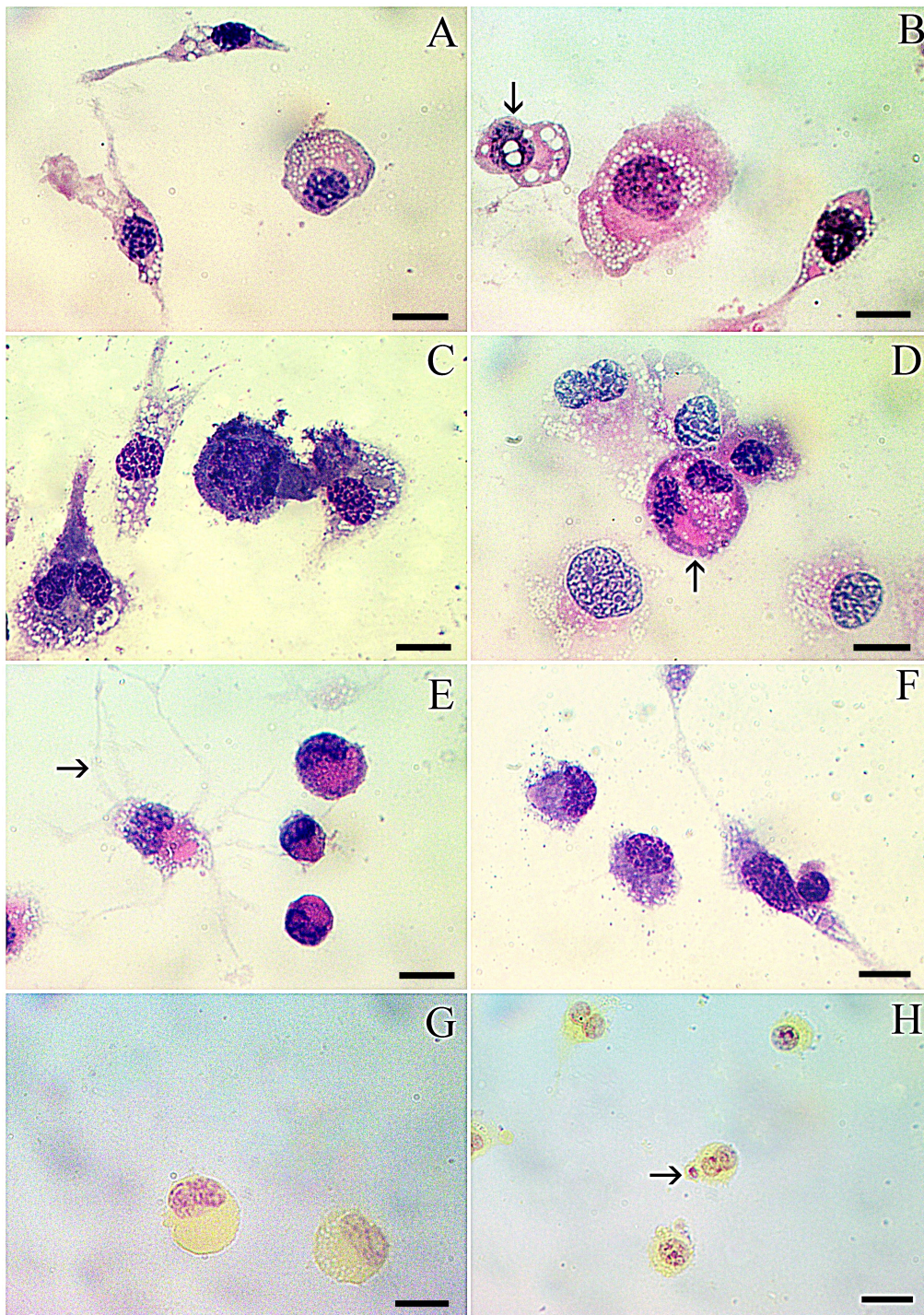


**Fig. 3. Morphological characteristics of the ASFV-infected human macrophages.** (A) Intact  $M\phi$  with vacuolized cytoplasm; Hematoxylin and Eosin (H-E) staining. Scale bar: 10  $\mu$ m. (B) Infected (24 hpi) with active ASFV enlarged  $M\phi$  with massive vacuolization, which includes nucleus (arrowed), H-E staining. Scale bar: 10  $\mu$ m. (C)  $M\phi$  incubated with inactive ASFV (48 hpi) severe vacuolization, Papanheim staining. Scale bar: 10  $\mu$ m. (D)  $M\phi$  incubated with inactive ASFV (48 hpi) severe vacuolization, cytoplasmic basophilia (arrowed), H-E staining. Scale bar: 10  $\mu$ m. (E) Infection (48 hpi) with active ASFV  $M\phi$  with mild vacuolization and pronounced pseudopodia (arrowed), H-E staining. Scale bar: 10  $\mu$ m. (F) Infection (48 hpi) with active ASFV  $M\phi$  with mild vacuolization and pronounced pseudopodia (arrowed), Papanheim staining. Scale bar: 10  $\mu$ m. (G) Infected (24 hpi) with active ASFV  $M\phi$  without viral factories, Feulgen staining. Scale bar: 10  $\mu$ m. (H) Infected (24 hpi) with active ASFV porcine alveolar macrophages with typical viral factory (arrowed), Feulgen staining. Scale bar: 10  $\mu$ m.

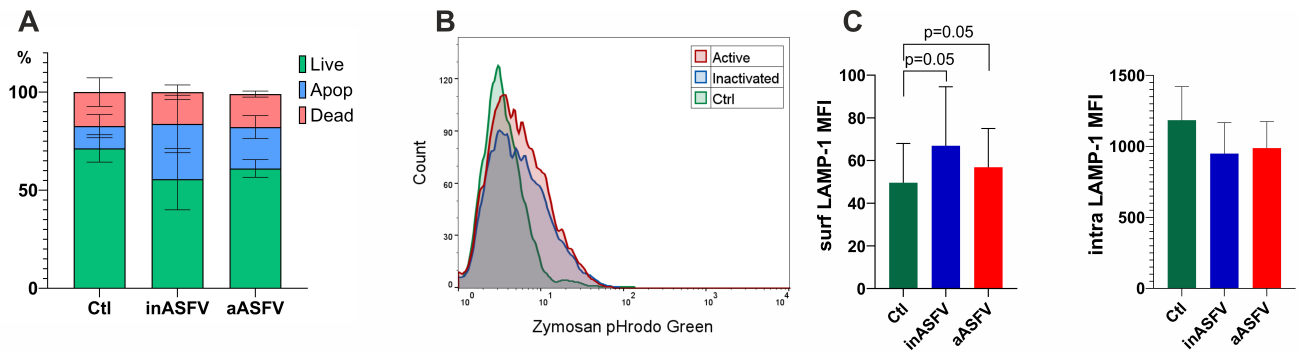


**Fig. 4. Functional tests of THP-1-derived M $\phi$ 0 cells infected with active virus (aASFV) and inactivated virus (inASFV) (n = 6).** (A) Percentage of live, apoptotic, and dead cells. (B) Representative overlay of histograms of pH changes in M $\phi$ 0 labeled with pHrodo-green-labeled Zymosan BioParticles. (C) Expression levels of surface and intracellular lysosome-associated membrane protein (LAMP-1) quantified as mean fluorescent intensity (MFI). Each experiment was repeated three times, and the results were averaged. Ctl, control.

teins on macrophages may also participate in the infection process [21]. In any case, the human CD163 receptor and/or other surface proteins of M $\phi$ 0 allow the virus to successfully enter the cells. Viral decapsidation occurs within mature endosomal compartments that express CD163. Once decapsidated, viral particles expose the inner envelope, which allows their interaction and subsequent fusion with the endosomal membrane. This leads to the release of naked cores into the cytosol, allowing viral replication to begin [21]. The ASFV is able to successfully complete this stage of the replication cycle in M $\phi$ 0 since only after that can it start the transcription of viral genes.

During viral replication, certain genes, such as early genes, are expressed before the viral DNA replication begins [8]. In human M $\phi$ 0 cells, this stage of viral replication is partially implemented: Several viral RNAs are not observed and/or occur at a very low level. At the same time, we did not reveal any difference in the functional state of transcription of viral genes, regardless of whether they are early or late genes.

The ASFV not only transcribes its own genes for the metabolism of viral replication but also has to suppress the host cell's defense mechanisms. In M $\phi$ 0 cells, the ASFV retains the functionality of a number of such mechanisms. The ASFV was unable to inhibit apoptosis in infected M $\phi$ 0 cells. Our experiments showed that apoptosis in aASFV-infected M $\phi$ 0 cells increased slightly in M $\phi$ 0 cells exposed to the virus.

When infected, M $\phi$  cells alter their cytokine/chemokine profile to defend the host. The presence of the viral genome triggers TLRs to stimulate the production of type I interferons such as IFN $\alpha$ , which may control early viral replication by promoting apoptosis and hampering the proliferation of virally infected cells. IFN $\alpha$ -induced activation of STAT1 and IRF1 is responsible for producing IL-10 by human monocytes/macrophages [22]. Following this trend, PAMs cultured with ASFV exhibited

elevated levels of IFN $\alpha$ , whereas THP-1-derived M $\phi$ 0 cells showed no difference in their production. The discrepancy may be due to the origin of cell types used in the study. IFN $\alpha$  helps shape the overall immune response by enhancing the phagocytic activity of macrophages, promoting their ability to engulf and digest virus particles and infected cells [23]. In the context of ASFV, IFN $\alpha$  can interfere with the ability of ASFV to replicate and spread within host cells, contributing to the containment of the infection [24]. Concomitant to the proinflammatory first line of defense triggered by TLR signaling, the immunoregulatory cytokine IL-10 is induced in macrophages. IL-10 is a key player in establishing and perpetuating viral persistence [25], and its increase is usually associated with high virulence [26,27]. Macrophages primarily produce IL-10 in response to TLR signaling as a form of feedback to limit the inflammatory response [28]. The lack of IL-10 in the supernatants from both PAMs and THP-1-derived M $\phi$ 0 cells indicates an early stage of infection with no apparent progression.

Our study found an upregulated expression of TLR3, which was recognized as a receptor in sensing the ASFV [16]. It was shown that the virus inhibits TLRs in pig macrophages as a strategy to avoid its recognition and efficiently replicate in these cells. For example, the *pI329L* gene was shown to target TIR-domain-containing adaptor-inducing interferon- $\beta$  (TRIF), a key MyD88-independent adaptor molecule, thus interfering with TLR3-stimulated activation [29]. Another gene, *pA276R*, inhibits IFN- $\beta$  induction via both the TLR3 and the cytosolic pathways by targeting IRF3 [30]. Given that ASFV replication occurs in the cytoplasm [31] and there is a lack of information about the activation of TLR3 from the cell surface, the upregulation of TLR3 in human macrophages might be reflective of the virus entering and being present in M $\phi$ 0 cells. TLR3 causes the activation of the TRIF-dependent downstream pathway, which in turn activates transcription fac-

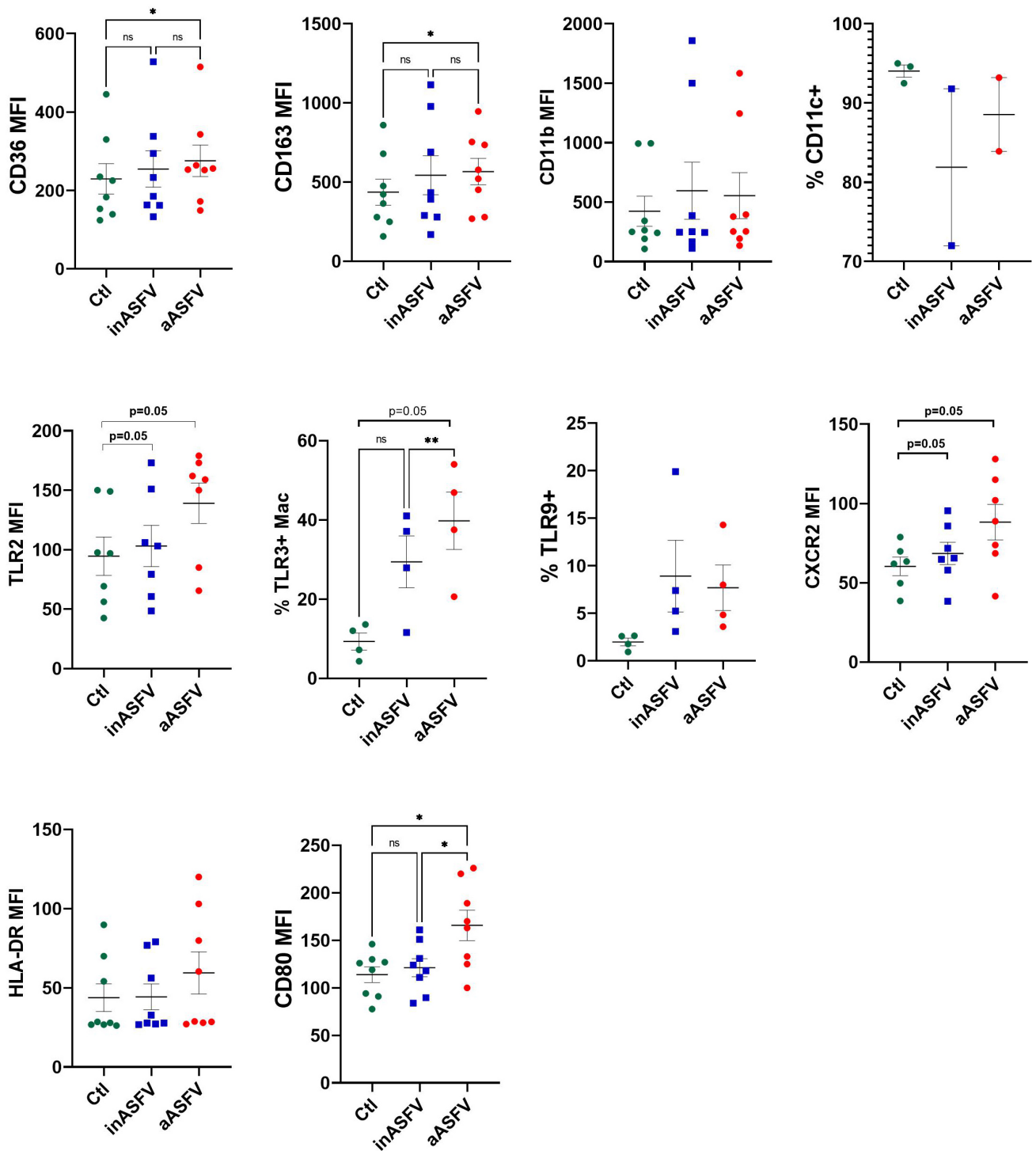


**Fig. 5. Differential expression of surface CD markers and Toll-like receptors (TLRs) by human THP-1-derived M $\phi$ 0 cells infected with active virus (aASFV) and inactivated virus (inASFV).** The graph shows the percentage of M $\phi$ 0 cells expressing TLR3 and TLR9 and mean fluorescent intensity (MFI) of CD11c, CD36, CD163, CD11b, CXCR2, TLR2, HLA-DR and CD80 on the surface of M $\phi$ 0 cells. Data are presented as the mean  $\pm$  standard error of the mean. \* $p < 0.05$ , \*\* $p < 0.01$ , ns, not significant. Each experiment was repeated three times, and the results were averaged.

tors, such as IRF3/7, NF- $\kappa$ B, and the activator protein 1 (AP-1), thus mediating the production of type I IFNs, proinflammatory cytokines, and chemokines, respectively [32]. The observed elevation in TNF- $\alpha$  production implies an ac-

tivated NF- $\kappa$ B response, at least within the context of our *in vitro* experimental model. Thus, upregulation of TLR3, the accessory molecule CD80 on macrophages lacking HLA-DR, may indicate a modulation of the antigen-presenting

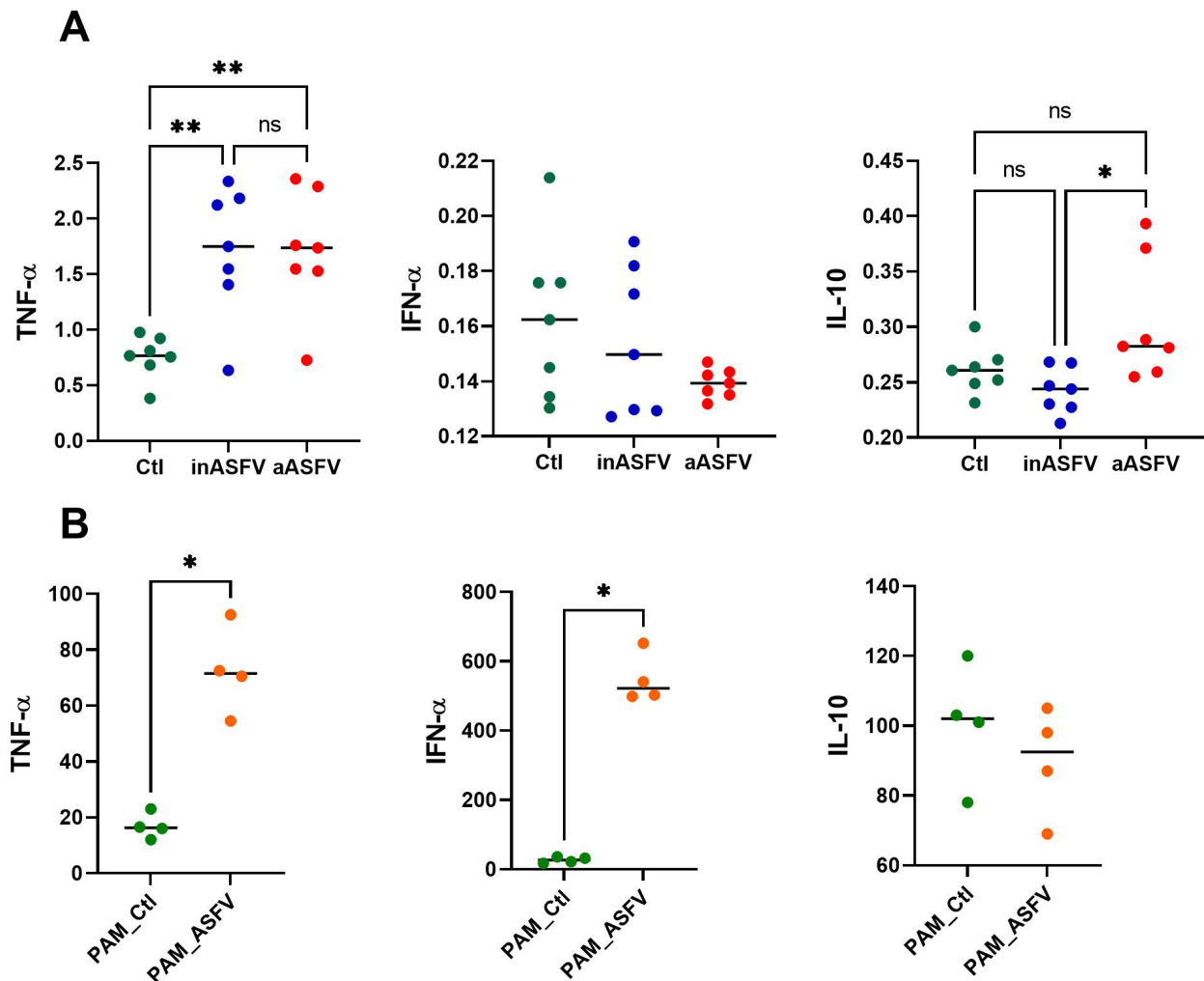


**Fig. 6. The effect of ASFV on production of cytokines TNF $\alpha$ , IFN- $\alpha$ , and IL-10.** (A) In culture supernatants of THP-1-derived M $\phi$ 0 cells infected with active virus (aASFV) and inactivated virus (inASFV) (n = 7). (B) In culture supernatants of PAMs (n = 4). Data are presented as the mean  $\pm$  standard error of the mean. \* $p$  < 0.05, \*\* $p$  < 0.01, ns, not significant. The statistical analysis of cytokine levels in the supernatants of THP-1-derived M $\phi$ 0 cells was conducted using one-way ANOVA, while the cytokine levels in the supernatants of PAMs were assessed using the Wilcoxon test. TNF $\alpha$ , tumor necrosis factor  $\alpha$ ; IFN- $\alpha$ , interferon- $\alpha$ ; IL-10, interleukin-10.

capabilities of the cells at the early stage of *in vitro* infection. Alternatively, it could be a component of the specific evasion strategy employed by the virus, providing additional confirmation of the virus's entry into macrophages.

The virulence of ASFV isolated in pigs was shown to be dependent on their ability to regulate the expression of cytokines derived from macrophages, which are important for the development of host protective responses through partially unknown mechanisms that are triggered by the virus in the early stages of cellular infection [3, 26]. However, in the human organism, viral replication is likely blocked at an early stage of infection of the target macrophages. Our study found that the virus elicited a significant response from M $\phi$ 0 cells that had been infected for 48 hours. Notably, increased surface expression of LAMP-1 indicates lysosome exocytosis of M $\phi$ 0 cells [33]. Engagement of co-stimulatory CD80, scavenger re-

ceptors, chemokine receptor CXCR2, and TLRs. In PAM cells, the virus can alter cellular functions rapidly within 24 hours of infection. When infected, this virus activity is slowed—the implementation is carried out up to 48 hpi.

Cytoplasmic viral factories, characteristic of ASFV, for example, on Feulgen-stained preparations [11], are not detected when infecting M $\phi$ 0 cells, which suggests that either the virus does not replicate or replicates in an insignificant undetectable amount. This coincides with the data obtained from the quantitative analysis of genome copies and infectious titers (Fig. 1).

Later stages of virus replication, such as ASFV egress, are very difficult to trace. Even if we assume that the virus can replicate with a decrease in infectious titers, this is unlikely, even though we showed the presence of the virus up to the third passage.

## 5. Conclusion

When examining the replication of the ASFV in M $\phi$ 0, it becomes evident that the virus can initiate the replication cycle by first entering human macrophages, losing its capsid, starting transcription of many of its proteins, and partially realizing their functions. ASFV in M $\phi$ 0 implements numerous functions to alter cell activity; however, the timing of these functional changes is slower in M $\phi$ 0 compared with susceptible cells, such as PAMs. Despite these alterations in cell activity, ASFV cannot complete the full replication cycle in human macrophages, which is evidenced by the absence of viral factories typically observed in sensitive cells and the decrease in infectious viral titers with each subsequent passage. These findings suggest that molecular limitations within human macrophages may at least partially restrict the complete replication of ASFV. Understanding the factors that hinder viral replication in M $\phi$ 0 can provide valuable insights into the host–virus interactions and the mechanisms underlying the resistance of human macrophages to the ASFV.

## Availability of Data and Materials

Data supporting the findings of this study are available from the corresponding author upon reasonable request.

## Author Contributions

ZK, GM were responsible for the conceptualization, data curation, writing – original draft, writing – review editing. LH, LA, AA, DP, HA were responsible for formal analysis. SG, DP, LH, HA, AA, LA, AP, SH were responsible for investigation. AP and SH also were responsible for editing process of the manuscript. All authors contributed to editorial changes in the manuscript. All authors read and approved the final manuscript. All authors have participated sufficiently in the work and agreed to be accountable for all aspects of the work.

## Ethics Approval and Consent to Participate

The studies were reviewed and approved by the Ethics Committee of the Institute of Molecular Biology NAS RA (IRB 00004079, 2013; Protocol N5 from 25 May 2018). The animal study protocol was approved by the Ethics Committee of the Institute of Molecular Biology NAS RA (IRB 06042021/1, 2021).

## Acknowledgment

Not applicable.

## Funding

This research received no external funding.

## Conflict of Interest

The authors declare no conflict of interest.

## Supplementary Material

Supplementary material associated with this article can be found, in the online version, at <https://doi.org/10.31083/j.fbl2904164>.

## References

- [1] Loh J, Zhao G, Presti RM, Holtz LR, Finkbeiner SR, Droit L, *et al.* Detection of novel sequences related to African Swine Fever virus in human serum and sewage. *Journal of Virology*. 2009; 83: 13019–13025.
- [2] Ogata H, Toyoda K, Tomaru Y, Nakayama N, Shirai Y, Claverie JM, *et al.* Remarkable sequence similarity between the dinoflagellate-infecting marine girus and the terrestrial pathogen African swine fever virus. *Virology Journal*. 2009; 6: 178.
- [3] Schäfer A, Franzoni G, Netherton CL, Hartmann L, Blome S, Blohm U. Adaptive Cellular Immunity against African Swine Fever Virus Infections. *Pathogens (Basel, Switzerland)*. 2022; 11: 274.
- [4] Enjuanes L, Cubero I, Viñuela E. Sensitivity of macrophages from different species to African swine fever (ASF) virus. *The Journal of General Virology*. 1977; 34: 455–463.
- [5] Wang T, Wang L, Han Y, Pan L, Yang J, Sun M, *et al.* Adaptation of African swine fever virus to HEK293T cells. *Transboundary and Emerging Diseases*. 2021; 68: 2853–2866.
- [6] Meloni D, Franzoni G, Oggiano A. Cell Lines for the Development of African Swine Fever Virus Vaccine Candidates: An Update. *Vaccines*. 2022; 10: 707.
- [7] Mlcochova P, Winstone H, Zuliani-Alvarez L, Gupta RK. TLR4-Mediated Pathway Triggers Interferon-Independent G0 Arrest and Antiviral SAMHD1 Activity in Macrophages. *Cell Reports*. 2020; 30: 3972–3980.e5.
- [8] Avagyan HR, Hakobyan SA, Poghosyan AA, Bayramyan NV, Arzumanyan HH, Abroyan LO, *et al.* African Swine Fever Virus Manipulates the Cell Cycle of G0-Infected Cells to Access Cellular Nucleotides. *Viruses*. 2022; 14: 1593.
- [9] Enjuanes L, Carrascosa AL, Moreno MA, Viñuela E. Titration of African swine fever (ASF) virus. *The Journal of General Virology*. 1976; 32: 471–477.
- [10] Hakobyan SA, Ross PA, Bayramyan NV, Poghosyan AA, Avetisyan AS, Avagyan HR, *et al.* Experimental models of ecological niches for African swine fever virus. *Veterinary Microbiology*. 2022; 266: 109365.
- [11] Karalyan ZA, Izmailyan RA, Abroyan LO, Avetisyan AS, Hakobyan LA, Zakaryan HS, *et al.* Evaluation of Viral Genome Copies Within Viral Factories on Different DNA Viruses. *The Journal of Histochemistry and Cytochemistry: Official Journal of the Histochemistry Society*. 2018; 66: 359–365.
- [12] Ginzinger DG. Gene quantification using real-time quantitative PCR: an emerging technology hits the mainstream. *Experimental Hematology*. 2002; 30: 503–512.
- [13] Yin JL, Shackel NA, Zekry A, McGuinness PH, Richards C, Putten KV, *et al.* Real-time reverse transcriptase-polymerase chain reaction (RT-PCR) for measurement of cytokine and growth factor mRNA expression with fluorogenic probes or SYBR Green I. *Immunology and Cell Biology*. 2001; 79: 213–221.
- [14] Cackett G, Portugal R, Matelska D, Dixon L, Werner F. African Swine Fever Virus and Host Response: Transcriptome Profiling of the Georgia 2007/1 Strain and Porcine Macrophages. *Journal of Virology*. 2022; 96: e0193921.
- [15] Rammensee HG, Singh-Jasuja H. HLA ligandome tumor antigen discovery for personalized vaccine approach. *Expert Review of Vaccines*. 2013; 12: 1211–1217.
- [16] Ayanwale A, Trapp S, Guabiraba R, Caballero I, Roesch F. New Insights in the Interplay Between African Swine Fever Virus and

- Innate Immunity and Its Impact on Viral Pathogenicity. *Frontiers in Microbiology*. 2022; 13: 958307.
- [17] McCarthy CG, Gouloupoulou S, Wenceslau CF, Spitler K, Matsumoto T, Webb RC. Toll-like receptors and damage-associated molecular patterns: novel links between inflammation and hypertension. *American Journal of Physiology. Heart and Circulatory Physiology*. 2014; 306: H184–H196.
- [18] Beldekas J, Teas J, Hebert JR. African swine fever virus and AIDS. *Lancet (London, England)*. 1986; 1: 564–565.
- [19] Schiedner G, Doerfler W. Insufficient levels of NFIII and its low affinity for the origin of adenovirus type 12 (Ad12) DNA replication contribute to the abortive infection of BHK21 hamster cells by Ad12. *Journal of Virology*. 1996; 70: 8003–8009.
- [20] Preuss MA, Lam JT, Wang M, Leath CA, 3rd, Kataram M, Mahasreshthi PJ, *et al.* Transcriptional blocks limit adenoviral replication in primary ovarian tumor. *Clinical Cancer Research: an Official Journal of the American Association for Cancer Research*. 2004; 10: 3189–3194.
- [21] Galindo I, Alonso C. African Swine Fever Virus: A Review. *Viruses*. 2017; 9: 103.
- [22] Ziegler-Heitbrock L, Lötzerich M, Schaefer A, Werner T, Frankenberger M, Benkhart E. IFN-alpha induces the human IL-10 gene by recruiting both IFN regulatory factor 1 and Stat3. *Journal of Immunology (Baltimore, Md.: 1950)*. 2003; 171: 285–290.
- [23] García-Nicolás O, Godel A, Zimmer G, Summerfield A. Macrophage phagocytosis of SARS-CoV-2-infected cells mediates potent plasmacytoid dendritic cell activation. *Cellular & Molecular Immunology*. 2023; 20: 835–849.
- [24] Fan W, Jiao P, Zhang H, Chen T, Zhou X, Qi Y, *et al.* Inhibition of African Swine Fever Virus Replication by Porcine Type I and Type II Interferons. *Frontiers in Microbiology*. 2020; 11: 1203.
- [25] Wilson EB, Brooks DG. The role of IL-10 in regulating immunity to persistent viral infections. *Current Topics in Microbiology and Immunology*. 2011; 350: 39–65.
- [26] Gil S, Spagnuolo-Weaver M, Canals A, Sepúlveda N, Oliveira J, Aleixo A, *et al.* Expression at mRNA level of cytokines and A238L gene in porcine blood-derived macrophages infected in vitro with African swine fever virus (ASFV) isolates of different virulence. *Archives of Virology*. 2003; 148: 2077–2097.
- [27] Gómez-Villamandos JC, Bautista MJ, Sánchez-Cordón PJ, Carrasco L. Pathology of African swine fever: the role of monocyte-macrophage. *Virus Research*. 2013; 173: 140–149.
- [28] Rojas JM, Avia M, Martín V, Sevilla N. IL-10: A Multifunctional Cytokine in Viral Infections. *Journal of Immunology Research*. 2017; 2017: 6104054.
- [29] de Oliveira VL, Almeida SCP, Soares HR, Crespo A, Marshall-Clarke S, Parkhouse RME. A novel TLR3 inhibitor encoded by African swine fever virus (ASFV). *Archives of Virology*. 2011; 156: 597–609.
- [30] Correia S, Ventura S, Parkhouse RM. Identification and utility of innate immune system evasion mechanisms of ASFV. *Virus Research*. 2013; 173: 87–100.
- [31] Wang N, Zhao D, Wang J, Zhang Y, Wang M, Gao Y, *et al.* Architecture of African swine fever virus and implications for viral assembly. *Science (New York, N.Y.)*. 2019; 366: 640–644.
- [32] Yang Q, Shu HB. Deciphering the pathways to antiviral innate immunity and inflammation. *Advances in Immunology*. 2020; 145: 1–36.
- [33] Haka AS, Barbosa-Lorenzi VC, Lee HJ, Falcone DJ, Hudis CA, Dannenberg AJ, *et al.* Exocytosis of macrophage lysosomes leads to digestion of apoptotic adipocytes and foam cell formation. *Journal of Lipid Research*. 2016; 57: 980–992.